Gamma-Ray Bursts: Electromagnetic Signal & Gravitational Wave emission

A. Corsi (Vesf fellow) & L. Piro (Iasf-INAF)

In collaboration with: **P. Rapagnani & F. Ricci (“La Sapienza”)**

LIGO-G060346-00-Z

GRBs: EM signal and GW

EM signal

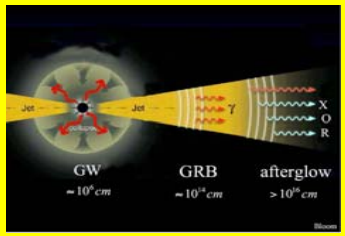

Progenitor models

GW emission

Source position and distance, trigger time and time window

Detecting GW

\+

Total energy output: hints on the disk mass

Nature of the progenitor

Amplitude of the GW signal: hints on the masses (e.g. chirp or mass ratio)

The EM signal

Gamma-Ray Bursts

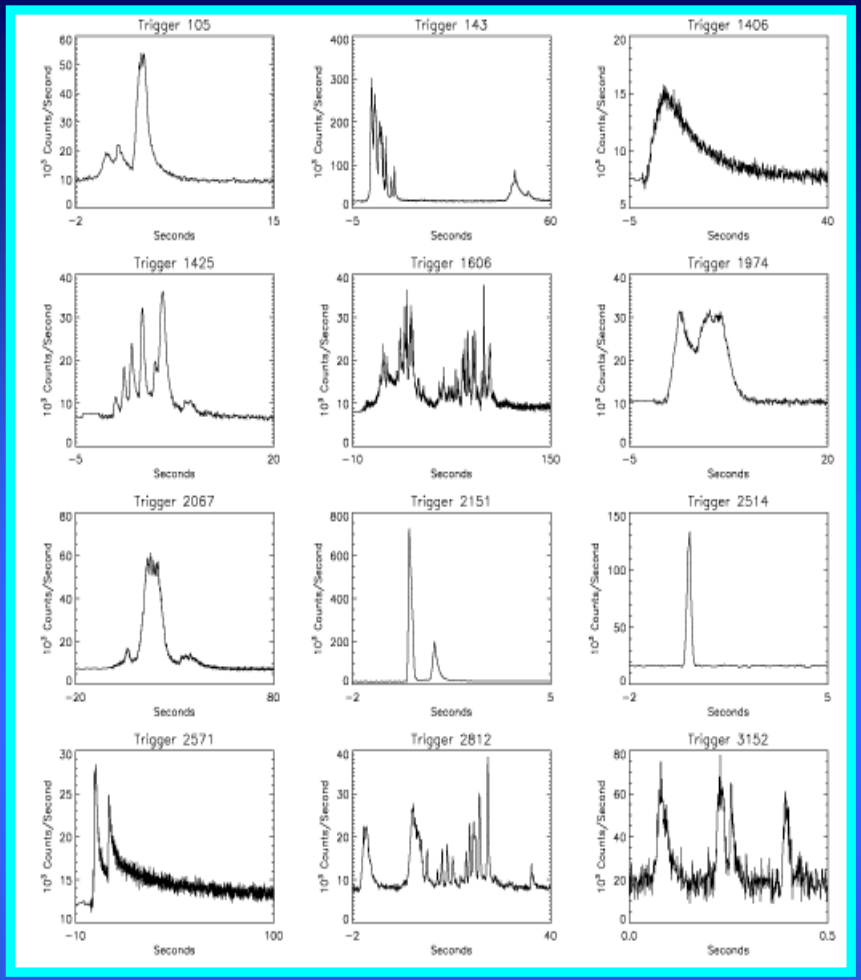

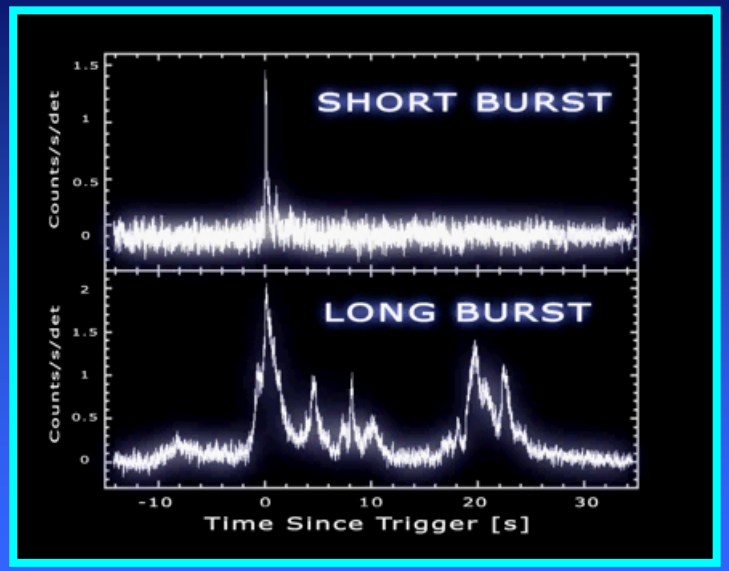

Two classes of bursts: short / long

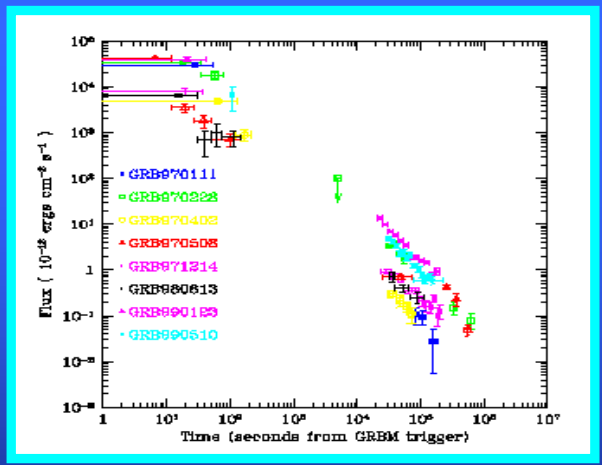

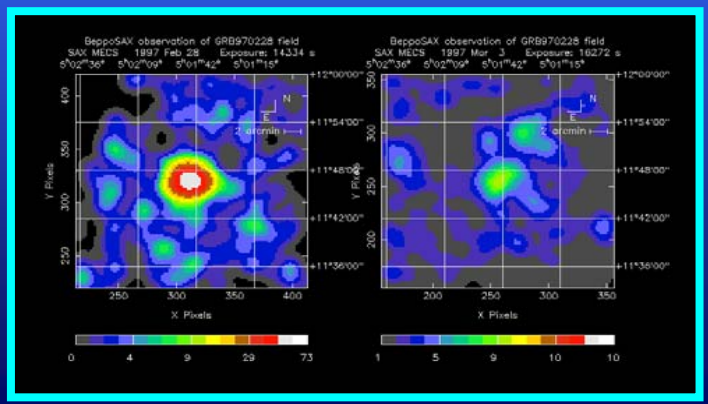

Prompt emission followed by an “afterglow” ($F \propto t^{-1.3}$), i.e. time decreasing multi-wavelength emission. Optical counterpart allows host detection and redshift measurements

GRBs: Short vs long

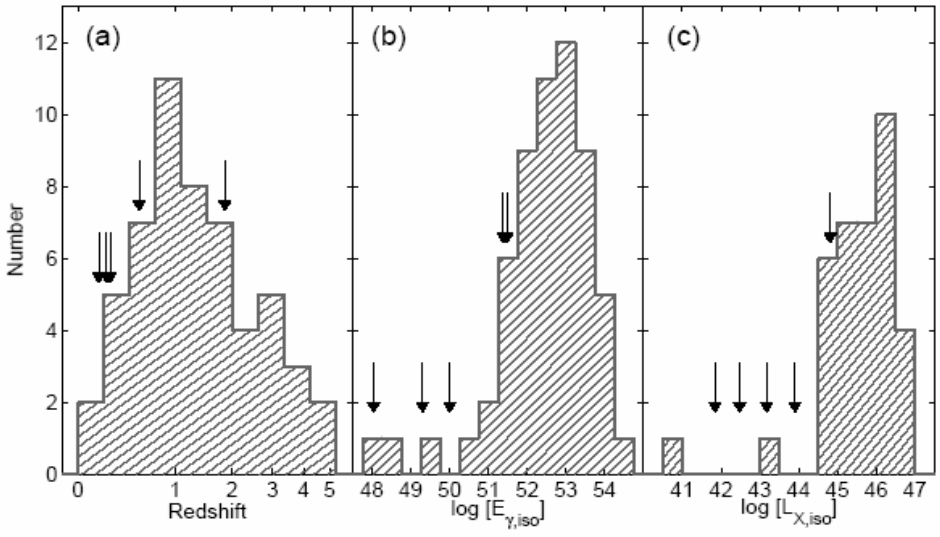

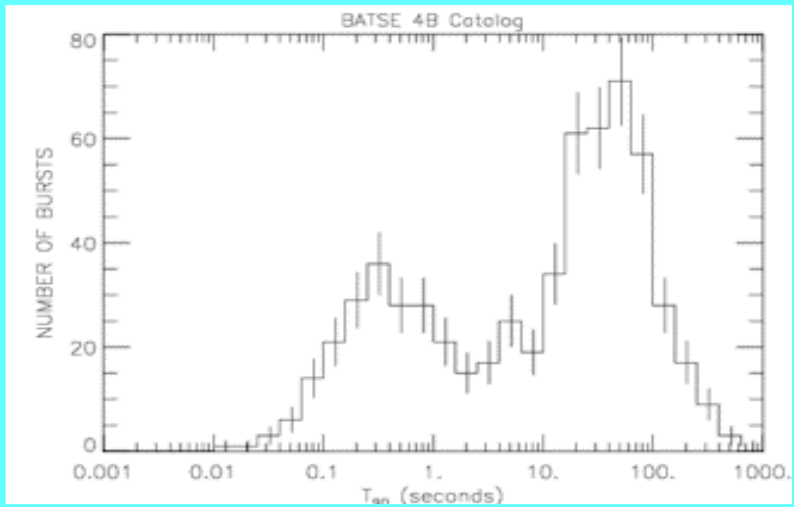

Short bursts: T_{90} < 2 s, recognized as a separate sub-class from long GRB

Berger, 2006, astro-ph/06042004

- sample of five short GRBs with precise or putative redshift:
0.16 < z < 1.8 (3/5 bursts at z < 0.3 - two more recent cases, z <1.7 & z=1.5-4.6(?));

- Isotropic γ-ray energies: $E_{\gamma,iso} \approx 1.1\times10^{48} - 3\times10^{51}$ erg: wide range **at the low end of the distribution for long GRBs;**

- X-ray afterglow luminosities: $L_{X,iso}(t=10hr) \approx 7.0\times10^{41} - 6.4\times10^{44}$ erg/s wide range, **at the low end of the distribution for long GRBs.**

The fireball model for gamma-ray bursts

The "fireball model": a GRB is produced when an ultra-relativistic ejecta from a central engine is stopped in the interactions between shells of different velocities (internal shocks, $d \sim 10^{14}$ cm) or with the external medium (external shocks, $d \geq 10^{16}$ cm). In those interactions, the kinetic energy of the relativistic flow is converted in internal energy of relativistic electrons that produce the observed radiation via synchrotron (and IC) emission.

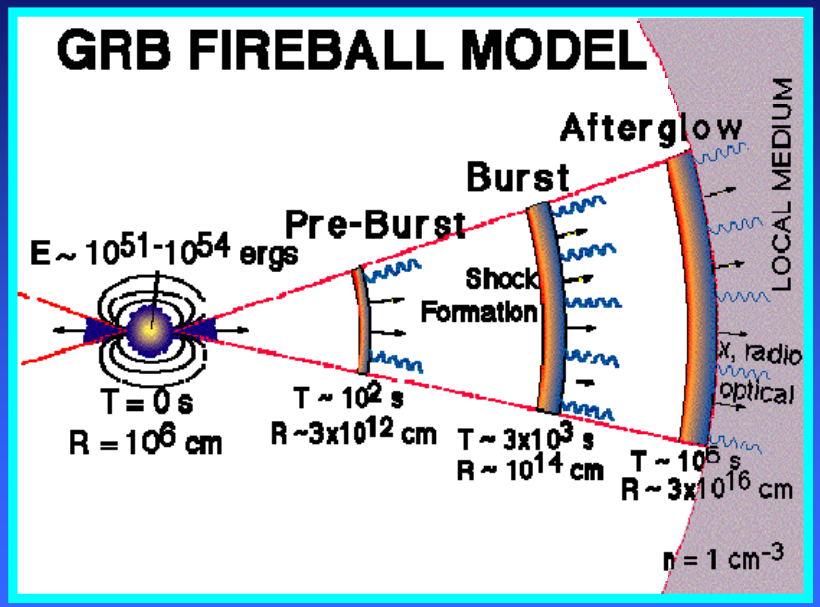

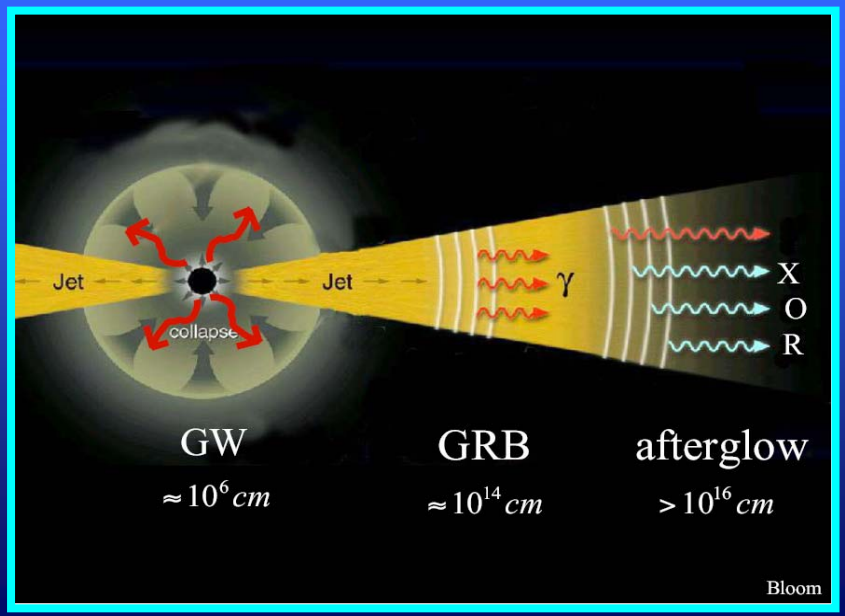

Nature of the inner engine: the GRB progenitor is electromagnetically hidden from direct observation because all the radiation is emitted at $d > 10^{13}$ cm. Although the lack of direct evidence, it is widely accepted that GRBs are the result of catastrophic events involving either compact stellar mergers (short GRBs) or massive stellar collapse (long GRBs). GWs should be emitted from the immediate neighborhood of the GRB central engine.

The progenitor: some more details

Long GRBs: the progenitor

Collapsar model (e.g. Woosley 1998):

- **"GRB as the birth cry of a BH": when the collapse of the iron core of a rotating massive progenitor proceeds directly to a BH formation, the stellar mantle falls into the newly formed BH and angular momentum slows the collapse along the equator, ultimately forming an accretion disk that, within a few seconds, launches particle jets along the rotation axis powering a GRB**

- **The jets pass through the outer shells of the star and combined with the vigorous winds of newly forged radioactive metals blowing off the disk inside, give rise to the supernova event**

- **Collisions among shells of the jet moving at different velocities, far from the explosion and moving close to light speed, create the GRB, which can only be seen if the jet points toward us**

http://www.nasa.gov/centers/goddard/news/topstory/2003/0319hete.html

Short GRBs: the progenitor

General picture:

Merger events of NS+NS or BH+NS systems widely favored:

- **Seems unlikely that typical energies of short GRBs set free during the dynamical merging; the following accretion phase in a postmerger system consisting of a central BH and a surrounding torus is much more promising**

- **BH-torus system geometry: relatively baryon-poor regions along the rotational axis ⇒ thermal energy release preferentially above the BH poles via e.g. ν anti-ν annihilation ⇒ can lead to collimated, highly relativistic jets of baryonic matter if thermal energy deposition rate per unit solid angle sufficiently large.**

- **γ-rays produced in internal shocks when blobs of ultra-relativistic matter in the jet collide with each other. When the jet hits the ISM, the afterglow is produced**

http://www.nasa.gov/mission_pages/swift/bursts/short_burst_nsu_multimedia.html

GRB: progenitor models and time duration

Both progenitor types result in the formation of a few solar mass BH, surrounded by a torus whose accretion can provide a sudden release of energy, sufficient to power a burst. But different natural timescales imply different burst durations:

- **LONG: death of massive stars ⇒ free-fall time of the material falling on the disk form outside,**

$$t_{ff} \approx 30s(M/10M_{\odot})^{-1/2} (R/10^{10}cm)^{3/2}$$

- **SHORT: coalescing compact objects ⇒ duration set by the viscous timescale of the gas accreting onto the newly-formed BH (short due to the small scale of the system)**

Constraining the progenitor: GRB-SN connection and host galaxies

- **GRB-SN connection supports the collapsar model for long GRBs:**

GRB 980425 (z 0.0085) and SN 1998bw - peculiar, more energetic than usual Type Ib/c supernova; using SN 1998bw as a template, other possible detection of reddened bumps in the optical afterglow light-curves after a time delay compatible with a supernova brightness rise-time, e.g. in GRB 980326, 970228, 000911, 990712, 011121, and 020405; GRB 030329 (z=0.169) and SN 2003dh - supernova light-curve reddened bump, in it a supernova spectrum of type Ib/c, delay between GRB and SN < 2d and compatible with both events being simultaneous; more recently: GRB 060218 (z=0.033) and SN2006aj - type Ic supernova, time origin within less than a 1 d from the GRB.

- **Nature of GRB hosts supporting the idea of a distinct population:**

Swift sample (up to the end of 2005): out of the 90 long GRBs, when a host was identified it was of an early type, usually a blue star-forming galaxy; out of 10 short GRB 4 of the hosts (GRB 040924, 050509b, 050724 and 050813) are elliptical galaxies, one (GRB 050709) is a nearby irregular galaxy, and one (GRB 050906) is a star-forming galaxy. All short hosts have SFR lower than the median for long GRB hosts. NS binaries: expected to be more abundant in old stellar population galaxies (as ellipticals) because of the long binary merger times (usually > 10^8 years). But more recent populations synthesis calculations reduced this so that compact mergers expected also in young, e.g. star-forming galaxies, although statistically most mergers expected in old galaxies.

The expected GW signal &VIRGO

Estimating the strains of GWs from GRB progenitor candidates

$M=(m_{1,\odot}\, m_{2,\odot})^{3/5}\,(m_{1,\odot}+m_{2,\odot})^{-1/5}=(m_{1,\odot})\, q^{-2/5}/(q+1)^{1/5}$ $\quad M=m_1+m_2$ $\quad \mu=m_1/(1+q)$

- **In-spiral:** $h_c(f) \sim 1.4\times10^{-21}\,(d/10\ \mathrm{Mpc})^{-1}\, M^{5/6}\,(f/100\ \mathrm{Hz})^{-1/6}$

  $f \le f_i \sim 1000\,[M/2.8M_\odot]^{-1}\ \mathrm{Hz}$

  Short GRBs, optimal filtering can be applied

- **Merger:** $h_c \sim 2.7\times10^{-22}\,(d/10\ \mathrm{Mpc})^{-1}\,(4\mu/M_\odot)\,F^{-1/2}(a)\,(\varepsilon_m/0.05)^{1/2}$

  Kobayashi & Meszaros 2003

  $f_i \le f \le f_q \sim 32\ \mathrm{kHz}\ F(a)\,(M/M_\odot)^{-1}$

  $E_m=\varepsilon_m\,(4\mu/M)^2\,M\,c^2$

  $F(a)=1-0.63\,(1-a)^{3/10}$

  Short & Long GRBs, order of magnitude estimate of h_c

- **Ring-down:** slowly damped mode, l=m=2, peaked at f_q and width Δf:

  $\Delta f \sim \pi f_q/Q(a)$, where $Q(a)=2(1-a)^{-9/20}$

  Short & Long GRBs, but frequency too high

  $h_c(f_q) \sim 2.0\times10^{-21}\,(d/10\ \mathrm{Mpc})^{-1}\,(\mu/M_\odot)\,[Q/14\,F]^{1/2}\,(\varepsilon_r/0.01)^{1/2}$

Typical values

$a \sim 0.98$ $\quad \varepsilon_m \sim 0.05$ $\quad \varepsilon_r \sim 0.01$

Kobayashi & Meszaros 2003

Detectability

Optimal filtering (in-spiral & ring down):

$\langle\rho^2\rangle_{opt}=4\int [h_c(f)\,(f\ S_h(f))^{-0.5}]^2\, d(\ln f)$

$\rho \propto (d/10\ \mathrm{Mpc})^{-1}\, M^{5/6} \ge 5$

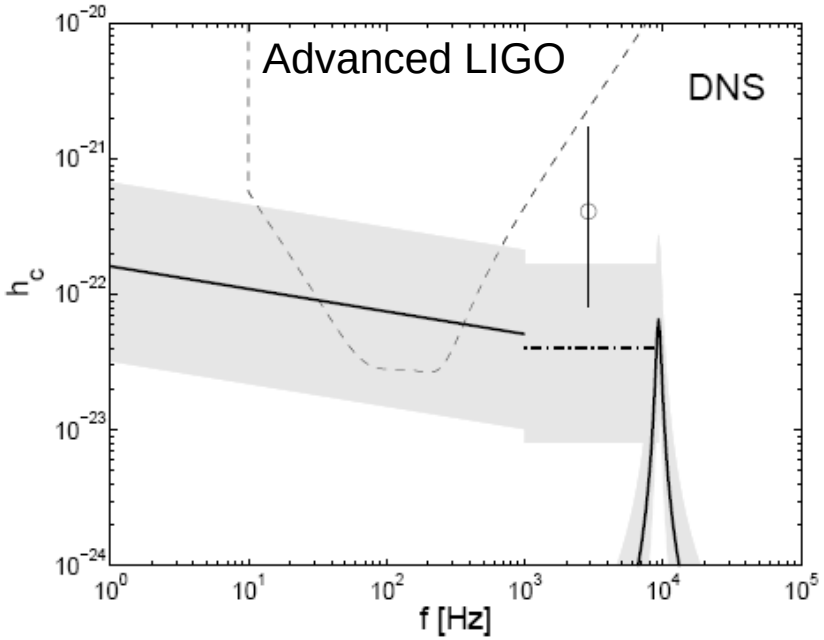

Fig. 1.— Double neutron stars: in-spiral (solid line), merger (dashed dotted line), bar (circle), ring-down(solid spike), see discussion in §3.1. $d = 220$Mpc, $m_1 = m_2 = 1.4M_\odot, a = 0.98, \epsilon_m = 0.05, m = m' = 2.8M_\odot, N = 10$ and $\epsilon_r = 0.01$.. Also shown is the advanced LIGO noise curve $\sqrt{fS_h(f)}$ (dashed curve). The shaded region and the vertical line reflect the uncertainty of the formation rate R in Table 1. The values of ϵ_m and ϵ_r are highly uncertain. The assumed values of $\epsilon_m = 0.05$ and $\epsilon_m = 0.01$ are rather optimistic. The presented strain in the merger, bar and ring-down phases in Figure 1-5 give order-of-estimates or the upper limits.

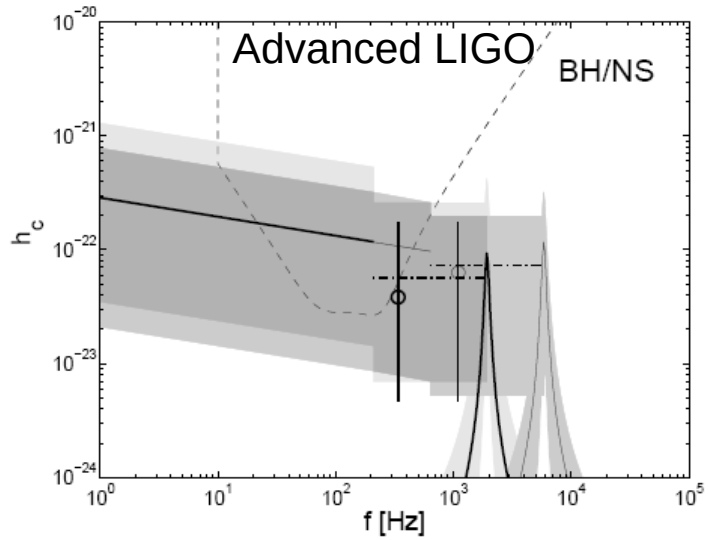

Fig. 2.— BH-NS, scenario a (thin lines and curve: $d = 170$Mpc, $m_1 = 3M_\odot, m_2 = 1.4M_\odot, a = 0.98, \epsilon_m = 0.05, m = 0.5M_\odot, m' = 4M_\odot, N = 10$ and $\epsilon_r = 0.01$) and scenario b (thick lines and curve: $d = 280$Mpc, $m_1 = 12M_\odot, m_2 = 1.4M_\odot, a = 0.98, \epsilon_m = 0.05, m = 0.5M_\odot, m' = 13M_\odot, N = 10$ and $\epsilon_r = 0.01$). In-spiral (solid line), merger (dashed dotted line), bar (circle) and ring-down(solid spike).

Kobayashi & Meszaros 2003

$$d \sim 230 \left(\frac{R}{\mathrm{Myr}^{-1}\mathrm{galaxy}^{-1}}\right)^{-1/3} \left(\frac{n_{glx}}{0.02\mathrm{Mpc}^{-3}}\right)^{-1/3} \mathrm{Mpc}$$

Table 1

	Formation Rate [$\mathrm{Myr}^{-1}\mathrm{galaxy}^{-1}$]		Distance [Mpc]	
	Standard	Range	Standard	Range
DNS	1.2	0.01-80	220	53-1100
BH-NS(a)	2.6	0.001-50	170	62-2300
(b)	0.55	0.001-50	280	62-2300
BH-WD	0.15	0.0001-1	430	230-4900
BH-He	14	0.1-50	95	62-490
Collapsar	630	10-1000	27	23-110

Fryer et al. 1999, Belczynski et al. 2002

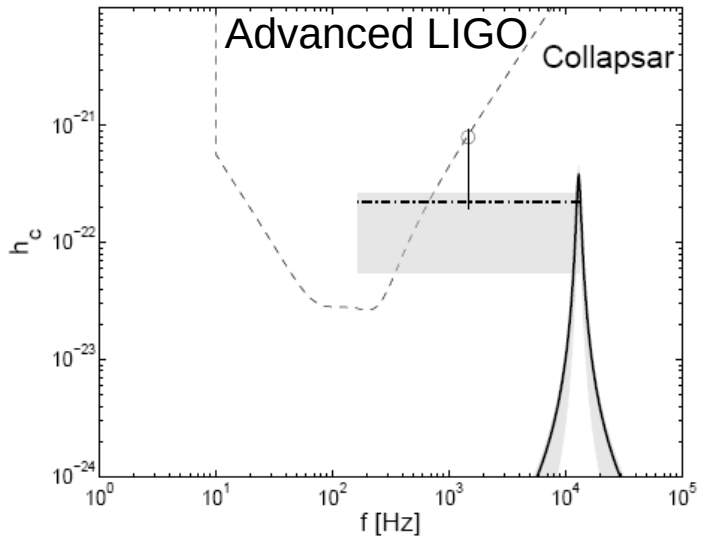

Fig. 5.— Collapsar: blob merger (dashed dotted line), bar (circle) and ring-down(solid spike). $d = 27$Mpc, $m_1 = m_2 = 1M_\odot, a = 0.98, \epsilon_m = 0.05, m = 1M_\odot, m' = 3M_\odot, N = 10$ and $\epsilon_r = 0.01$, see discussion in §3.5.

Characteristic GW amplitude from GRB candidate progenitors compared with the VIRGO noise curve $[f\, S_h(f)]^{1/2}$

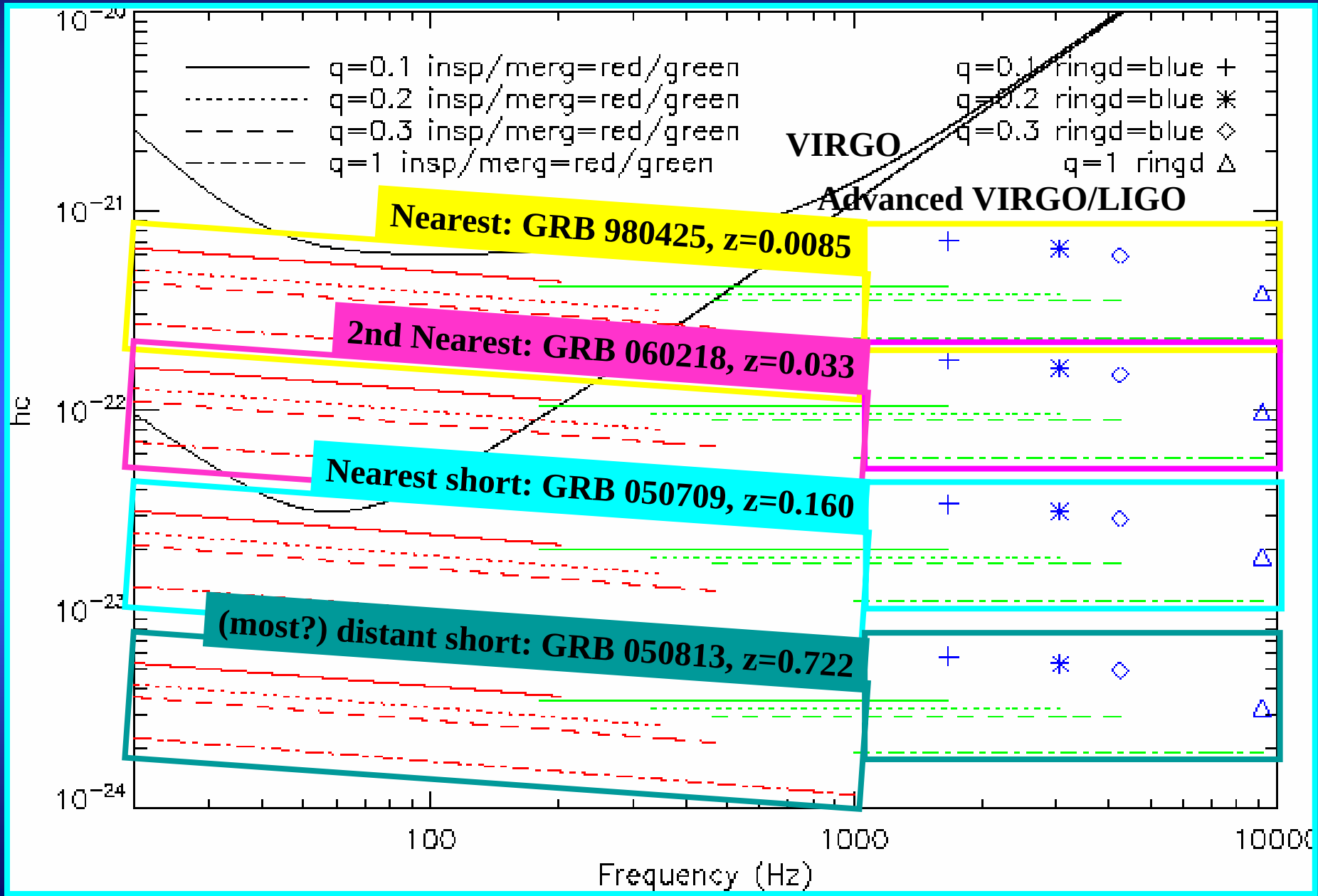

Some numbers for VIRGO: S/N in the inspiral

	m1= 1.4 m2= 14 q= 0.1 *M*= 3.45 μ= 1.27 M= 15.4 ffs (Hz)=182 ffm (Hz)=1673 fr (Hz)=1673	m1=1.4 m2=7 q=0.2 *M*=2.57 μ=1.17 M=8.4 ffs (Hz)=333 ffm (Hz)=3067 fr (Hz)=3067
z=0.0085 dl(Mpc)=37	(S/N)=2.2 (S/N)adv=38	(S/N)=1.8 (S/N)adv=30
z=0.033 dl(Mpc)=145	(S/N)=0.55 (S/N)adv=10	(S/N)=0.47 (S/N)adv=7.5
z=0.16 dl(Mpc)=765	(S/N)=0.10 (S/N)adv=1.8	(S/N)=0.089 (S/N)adv=1.4
z=0.722 dl(Mpc)=4424	(S/N)=0.018 (S/N)adv=0.31	(S/N)=0.015 (S/N)adv=0.25

LIGO-I and VIRGO: best fit model to current observations, given that Swift detects □ 10 Short GRBs per year ⇒ expected rate of simultaneous detections of short GRBs and GW is □ 0.3[0.1] yr^{-1} (Nakar et al. 2006).

	m1=1.4 m2=4.7 q=0.3 *M*=2.1 μ=1.1 M=6.1 ffs (Hz)=461 ffm (Hz)=4247 fr (Hz)=4247	m1=1.4 m2=1.4 q=1 *M*=1.2 μ=0.7 M=2.8 ffs (Hz)=1000 ffm (Hz)=9202 fr (Hz)=9202
	(S/N)=1.6 (S/N)adv=25	(S/N)=1.1 (S/N)adv=16
	(S/N)=0.42 (S/N)adv=6.5	(S/N)=0.27 (S/N)adv=4.0
	(S/N)=0.079 (S/N)adv=1.2	(S/N)=0.051 (S/N)adv=0.77
	(S/N)=0.014 (S/N)adv=0.21	(S/N)=0.0088 (S/N)adv=0.13

Linking EM signal and GW emission: time window

Relevant timescales

- The emitted gravitational waves are in the frequency band accessible to VIRGO & LIGO only for the last few minutes of inspiral (e.g. Cutler & Flanagan 1994);

- t_{ns} : time to form the BH accretion disk torus, i.e. time to form a BH from the NS. In a NSB the hypermassive NS should escape collapse for a sufficiently long time to form accretion torus; but collapse of the hot neutrino radiating NS should not be delayed too much because the non-relativistic expanding outflow of brayonic matter seriously endanger s the subsequent formation of a GRB jet (Oechslin & Janka 2006):
$E / M_{swept} c^2 = E / [(dM_{wind}/dt)\, t_{ns} c^2] > \Gamma_0$ where $E = E_{\gamma,iso}\, f_\Omega / f_4$
Typically $dM_{wind}/dt \sim 10^{-3}$-$10^{-5}\, M_\odot\, s^{-1}$, and $t_{ns} <$ 1-100 ms

- Simulated launch + evolution of relativistic jets driven by thermal energy deposition (e.g. ν anti-ν annihilation) near BH accretion torus systems: after 100 ms of constant energy supply (i.e. $t_{acc} \sim$ 100 ms), the fireball is at d ~ 3×10^9 cm. Standard fireball model: GRB produced at d >10^{13} cm ⇒ another 400 ms after the central engine supply shut off are needed to reach typical internal shock distances (Aloy et al. 2004).

Δt < 1 s between merger and a short GRB
Δt ~ 60 s safe

Linking EM signal and GW emission: torus mass vs mass ratio

Torus formation in NS-BH mergers

Once the disk is formed, the GRB energy output depends on its initial mass

e.g. Lee et al. (2005): simulating the dynamical evolution of the disk from BH-NS pairs (Lee 1999) covering the typical time duration of short GRBs. From the calculated neutrino luminosities, assuming an efficiency of 1% for the total energy deposition that could drive a relativistic outflow through ν anti-ν annihilation and the GRB duration, one can derive the total energy deposition, which turns out to be roughly independent of the inferred duration, which increases with decreasing disk viscosity since the overall evolution is slower. Instead, it strongly depends on the disk mass:

$E \sim 10^{49}$ erg $(M_{disc}/0.03M_{\odot})^2$

DISK FORMATION IN BH-NS MERGERS

M_{NS} (M_{BH})	Γ	m_d ($M_\odot$)	m_{tail} ($M_\odot$)
0.3	5/3	0.03	0.05
0.2	5/3	0.03	0.05
0.1	5/3	...	0.01
0.3	2.0	0.04	0.1
0.2	2.0	0.03	0.1
0.1	2.0	...	0.02

$M_{NS}=1.4M_{\odot}$

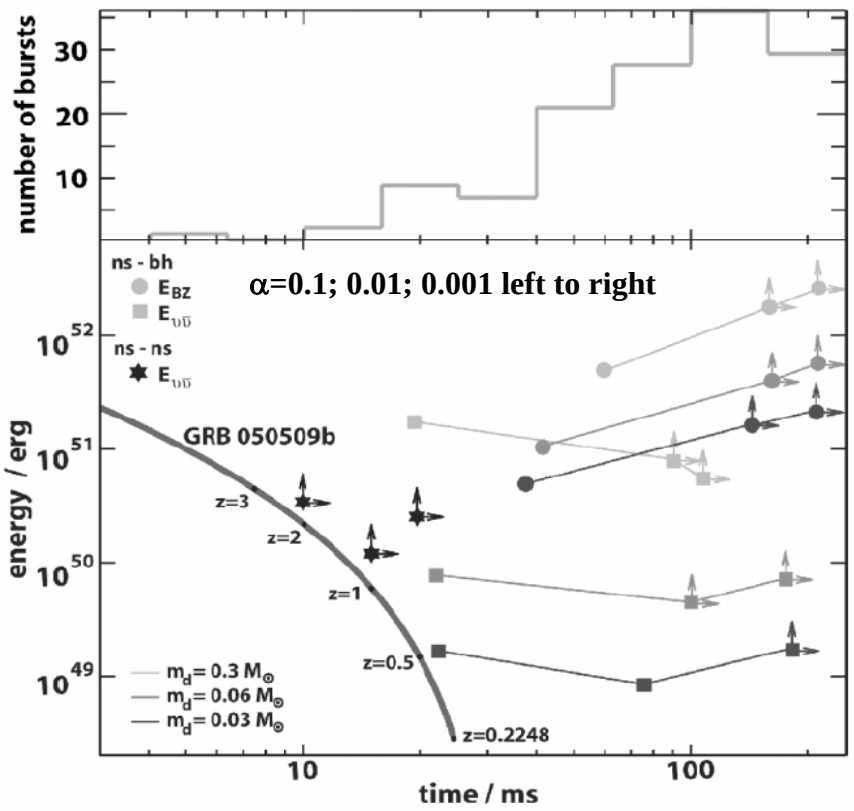

Torus formation in NS mergers

Merger dynamics largely dependent on the mass ratio q of the binary (Oechslin & Janka 2006):

GRB	z	t_γ	$E_{\gamma,\mathrm{iso}}$	M_{acc}	$\dot{M}_{\mathrm{acc}}$
Unit		sec.	ergs	$M_\odot$	$\frac{M_\odot}{\mathrm{s}}$
050509b	0.225	0.033	4.5×10^{48}	2.5×10^{-3}	0.08
050709	0.160	0.060	6.9×10^{49}	3.8×10^{-2}	0.6
050724	0.258	2.4	4.0×10^{50}	2.2×10^{-1}	0.09
050813	0.722	0.35	6.5×10^{50}	3.6×10^{-1}	1.0

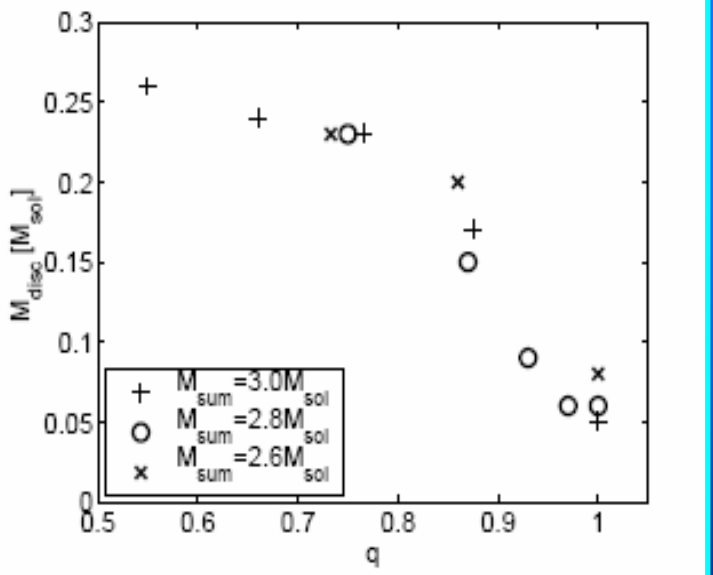

Figure 2. Disc masses versus mass ratio q for all non-zero temperature runs.

- **q<1: less massive but slightly larger star tidally disrupted and deformed into an enlongated primary spiral arm which is mostly accreted onto the more massive companion. Its tail, however, contributes a major fraction to the subsequently forming thick disk/torus around a highly deformed and oscillating central remnant.**

- **q~1 and ~ equally sized stars: both stars tidally stretched but not disrupted and directly plunge together into a deformed merger remnant.**

The disk mass is around 0.05 $M_\odot$ for q=1 and 0.26 $M_\odot$ for q=0.55.

Connection disk mass & energy output

Linking $E_{\gamma,iso}$ of a GRB to the energy output from the central engine and the mass M_{acc} accreted on the BH (during the phase when neutrino emission from the accreted torus is sufficiently powerful to drive the jets): chain of efficiency parameters corresponding to the different steps of physical processes between the energy release near the BH and the γ-ray emission at distances of ~ 10^{14} cm:

Directly measured: GRB prompt emission

$$E_{\gamma,iso} = f_1 f_2 f_3 f_\Omega^{-1} f_4 M_{acc} c^2$$

Disk mass: depends on the mass ratio q ⇒ enters in the in-spiral GW signal (chirp mass)

Efficiency at which accreted rest mass energy can be converted to neutrino emission

Conversion efficiency of ν anti-ν to e^+e^- pairs

Fraction of e^{+-}-photon fireball energy which drives the ultra-relativisitc outflow with $\Gamma > 100$

$f_\Omega = 2\Omega_{jet}/4\pi = 1-\cos\theta_{jet}$

Fraction of the sky covered by the two polar jets with semi-opening angles θ_{jet} and solid angles Ω_{jet}: afterglow light curve

Fraction of ultra-relativistic jet energy emitted in γ-rays via dissipative shocks when optically thin conditions are reached: broad-band afterglow modeling + prompt emission

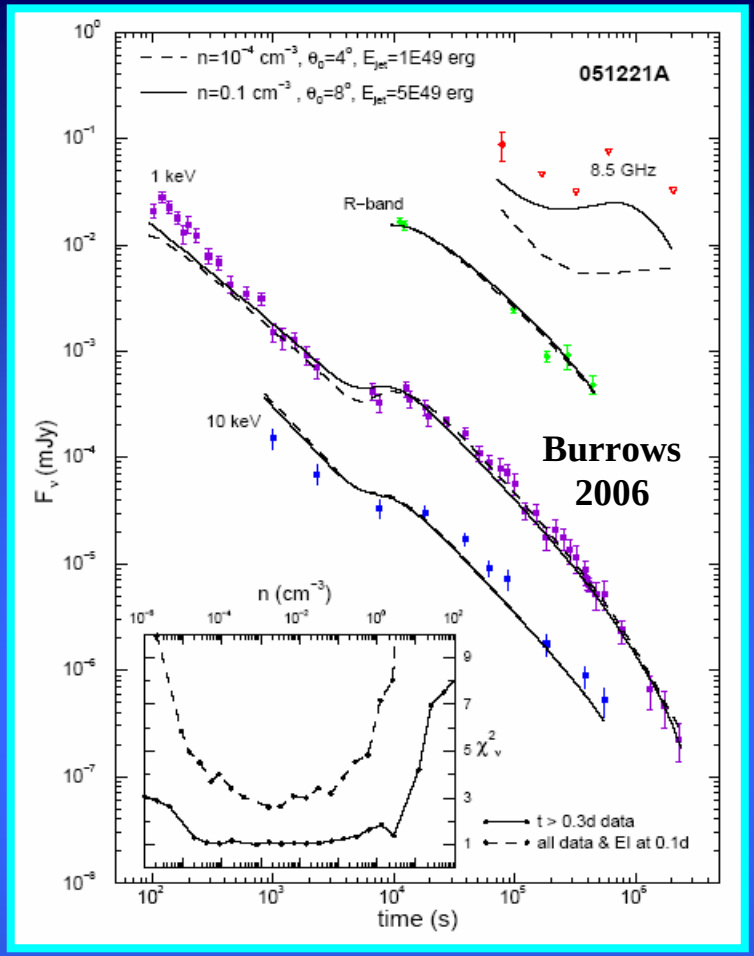

Fitting broad-band light curves: allows determination of blast wave kinetic energy (E) using the standard synchrotron model. Other parameters: n, ε_e and ε_B. The last two depend only on the micro-physics of the afterglow, while n (and E) should be different for long and short bursts if they are indeed associated with two distinct classes of progenitors, one short-lived and the other long-lived.

Jet opening angle and shocks efficiency from the afterglow EM signal

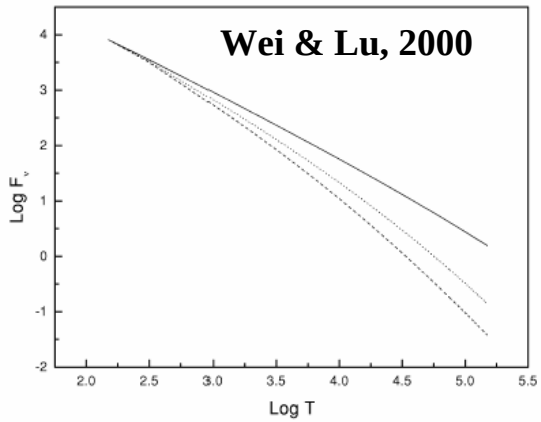

FIG. 1.—Afterglow light curves for different initial opening angles. The solid, dotted, and dashed lines represent the cases where $\theta_0 = 0.1$, 0.0174, and 0.01, respectively.

$$t_{\rm jet} \approx 6.2(E_{52}/n_1)^{1/3}(\theta_0/0.1)^{8/3}\ {\rm hr}$$

If the observer's l.o.s is inside the angle of the jet and $\Gamma^{-1} < \theta_j$, the light-cone is inside the jet boundary (causally disconnected) and the observer is unaware of what is outside the jet: spherical assumption valid. As the ejecta is decelerated: $\Gamma^{-1} > \theta_j$ and the dynamics changes, giving rise to the achromatic light curve breaks.

TABLE 1. Physical Properties of SHBs

	050709	050724	051221
Redshift	0.160	0.257	0.546
$E_{\gamma,\rm iso}$ (erg)	6.9×10^{49}	4.0×10^{50}	2.4×10^{51}
$E_{\rm KE,iso}$ (erg)	1.6×10^{48}	1.5×10^{51}	1.4×10^{51}
n (cm^{-3})	~ 0.01	~ 0.1	$\sim 10^{-3}$
ε_e	~ 0.3	~ 0.04	~ 0.3
ε_B	~ 0.3	~ 0.02	~ 0.1
θ_j (deg)	14	9	> 13
f_b	0.03	0.01	> 0.03
E_γ (erg)	2.1×10^{48}	4.5×10^{48}	$(6-240)\times10^{49}$
$E_{\rm KE}$ (erg)	5.0×10^{48}	1.7×10^{49}	$(4-140)\times10^{49}$
Reference	[20]	[18]	[26]

Berger, 2006

Conclusions & Work in progress

Combining the EM and GW signal can help understanding. Detecting the associated GW signal is the only way to have a conclusive evidence that our progenitor model are correct.

- **Focusing attention on the study of short-hard bursts: much more promising than long one to detect associated GW emission;**
- **Currently developing a code to model the expected afterglow emission in the standard fireball model to constrain its parameters (this gives E, jet) by fitting the afterglow data;**
- **Search for coincidence in the VIRGO data (in collaboration with the Rome VIRGO group;**

... thanks for Your attention!